J Mol Model (2010) 16:155–161
DOI 10.1007/s00894-009-0520-3

SHORT COMMENTS

Generation of a 3D model for human GABA transporter hGAT-1 using molecular modeling and investigation of the binding of GABA

Thomas Wein · Klaus T. Wanner

Received: 17 December 2008 / Accepted: 8 April 2009 / Published online: 9 June 2009

Abstract A three-dimensional model of the human Na^+/Cl^--dependent γ-aminobutyric acid (GABA) transporter hGAT-1 was developed by homology modeling and refined by subsequent molecular modeling using the crystal structure of a bacterial homologue leucine transporter from *Aquifex aeolicus* ($LeuT_{Aa}$) as the template. Protein structure quality checks show that the resulting structure is particularly suited for the analysis of the substrate binding pocket and virtual screening experiments. Interactions of GABA and the substrate binding pocket were investigated using docking studies. The difference of 6 out of 13 substrate interacting side chains between hGAT-1 and $LeuT_{Aa}$ lead to the different substrate preference which can be explained using our three-dimensional model of hGAT-1. In particular the replacement of serine 256 and isoleucine 359 in $LeuT_{Aa}$ with glycine and threonine in hGAT-1 seems to facilitate the selection of GABA as the main substrate by changing the hydrogen bonding pattern in the active site to the amino group of the substrate. For a set of 12 compounds flexible docking experiments were performed using LigandFit in combination with the Jain scoring function. With few exceptions the obtained rank order of potency was in line with experimental data. Thus, the method can be assumed to give at least a rough estimate of the potency of the potential of GABA uptake inhibitors.

T. Wein · K. T. Wanner (✉)
Department of Pharmacy, Center for Drug Research,
Ludwig-Maximilians-University Munich,
Butenandtstr. 7–13,
81377 Munich, Germany
e-mail: klaus.wanner@cup.uni-muenchen.de

Keywords Docking · Homology modeling · GABA · GABA transporter · GAT-1

Introduction

The sodium- and chloride-dependent γ-aminobutyric acid (GABA) transporter hGAT-1 is the most important GABA transporter out of four identified using molecular cloning techniques [1]. Unless otherwise specified, we will use the nomenclature introduced by Borden et al. [2] and Guastella et al. [3] for the human GABA transporters who referred to them as GAT-1, BGT-1, GAT-2, and GAT-3. hGAT-1 is essential for the termination of neurotransmission by removing GABA from the synaptic cleft. Other important members of the family of sodium and chloride dependent neurotransmitter transporters (SLC6) are specialized to transport other neurotransmitters like glycine, dopamine, norepinephrine, or serotonine [4–6]. The recent determination of the crystal structure of a prokaryotic Na^+/Cl^--dependent leucine transporter from *Aquifex aeolicus* ($LeuT_{Aa}$) [7] opened the possibility of understanding the structure-function relationship for this important transporter family. Distinct differences among important residues forming the active site are critical for the different substrate selectivity of this class of transporters [7–9]. Recently a 3D model for hGAT-1 has been published [10]. It is based on the alignment originally put forth by Yamashita et al. To differentiate between active and inactive compounds docking and subsequent molecular dynamics calculations are used. Being time consuming, this limits this model to the screening of selected ligands or to small compound libraries.

Materials and methods

Homology modeling and structure refinement

The protein sequence for the human hGAT-1 transporter protein was obtained from the Swiss-Prot database [11] (accession number P30531). The sequence and structure of $LeuT_{Aa}$ was obtained from the RCSB protein data bank [12] at 1.65 Å resolution (PDB ID 2A65). For generating the hGAT-1 structure we took the alignment from Beuming et al. [9]. This alignment has been refined using membrane protein-specific algorithms and by considering experimental data. Accordingly, it can be assumed to be the more reliable starting point for the generation of hGAT-1 models than the previously published alignment by Yamashita et al. [7]. Residues missing in the PDB file of $LeuT_{Aa}$ (Met1, Glu2, Val3, Lys4, Asn133, Ala134, Leu516, Val517, Pro518, and Arg519) and residues at the C and N termini of hGAT-1 which could not be aligned were dismissed for structure building.

Using the aforementioned sequence alignment from Beuming et al. in Fig. 1, three dimensional models of hGAT-1 were built by homology modeling using the MODELLER8v1 software with the default parameters [13]. The two sodium ions which are located directly in the active site were copied as ligands into the new models. Ten models were built and the best model was determined by the lowest value of the MODELLER objective function. Further energy minimization to avoid overlapping atoms and to adopt the binding site to GABA was carried out using GROMACS 4.0 [14, 15] utilizing the GROMOS96 force field [16]. For non-bonded interactions the PME method was used [17], the positions of the backbone atoms were restrained and only the side-chain atoms were allowed to move. One GABA molecule was preliminary docked into the selected hGAT-1 model and the complex was minimized in a box of water molecules to avoid unwanted side-effects of an in-vacuo simulation. Additional simulated annealing by heating up the system during 5 ps of MD to 310K, equilibrate it for 10 ps and cool it down to 0 K in 10 ps was performed in order to let the protein better adapt to GABA as ligand. The final structures were evaluated with PROCHECK [18] and Profiles-3D [19].

Docking of ligands

Charges and protonation for the protein were assigned using the CFF force field [20]. The binding site was assigned manually using the Binding Site Tools in Discovery Studio. For docking studies of selected ligands (Table 1), the ligand molecules were imported as 2D MDL Isis files into Discovery Studio and converted into 3D

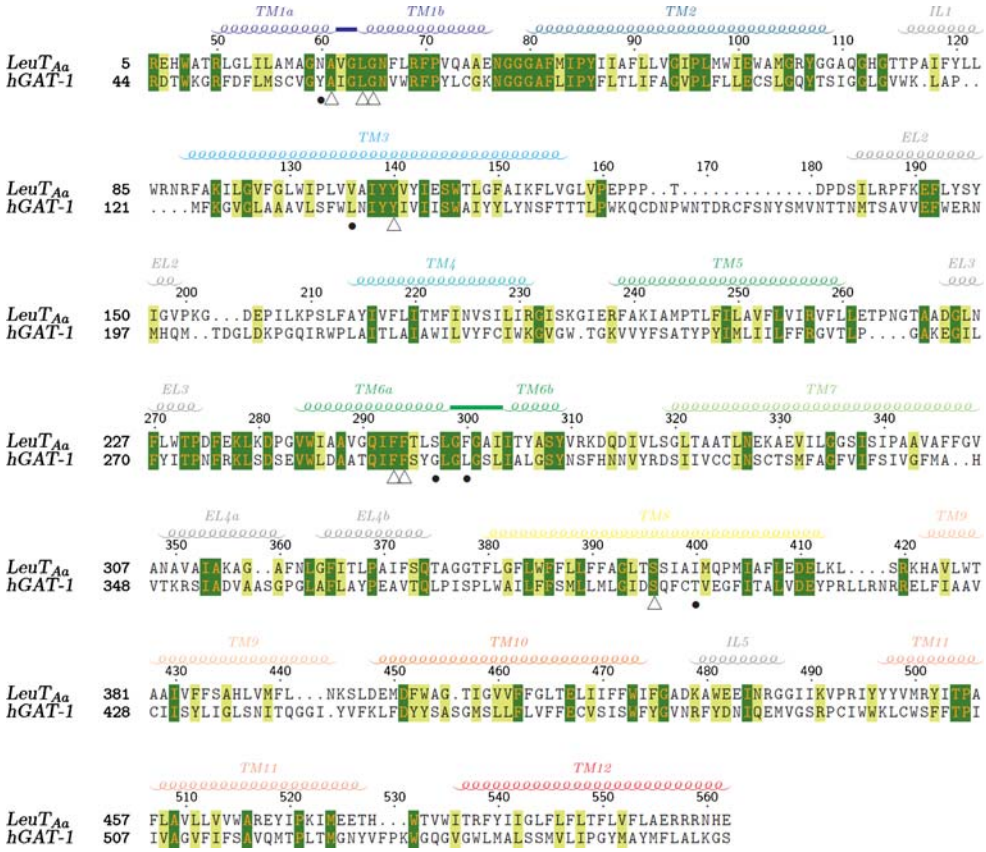

Fig. 1 The alignment of GAT-1 with $LeuT_{Aa}$. Numbering and labels for secondary structure elements are for hGAT-1. Identical residues in the active site are marked with triangles, different residues in the active site with filled circles. Figure was generated with TexShade

Table 1 Comparison of Jain scoring values and mGAT-1 uptake data [pIC50]. Table is ordered by mGAT-1 pIC50 values

Number	Compound	Structure	Jain Score	mGAT-1 (pIC50)
1	4-aminobutanoic acid (GABA)	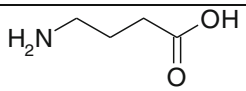	5.17	5.136
2	(*R*)-piperidine-3-carboxylic acid ((*R*)-nipecotic acid)	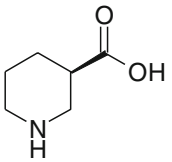	4.94	5.074
3	(*E*)-4-aminobut-2-enoic acid (*trans*-4-amino-crotonic acid)	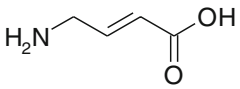	4.83	4.975
4	1,2,5,6-tetrahydropyridine-3-carboxylic acid (guvacine)	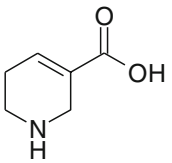	3.83	4.868
5	(*S*)-4-amino-2-hydroxybutanoic acid	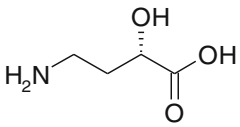	5.46	4.543
6	pyrrolidine-3-carboxylic acid (β-proline)	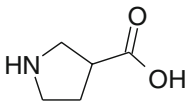	4.04	4.169
7	(*S*)-piperidine-3-carboxylic acid ((*S*)-nipecotic acid)	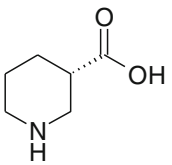	3.3	4.126
8	2-[(*R*)-pyrrolidin-2-yl]acetic acid ((*R*)-homoproline)	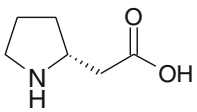	4.95	3.616
9	2-[(*S*)-pyrrolidin-2-yl]acetic acid ((*S*)-homoproline)	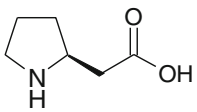	3.38	3.387
10	(*Z*)-4-aminobut-2-enoic acid (*cis*-4-amino-isocrotonic acid)	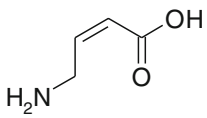	2.5	2.986
11	3-aminopropanoic acid (β-alanine)	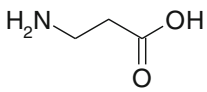	1.53	2.594
12	2-aminoethanesulfonic acid (taurine)	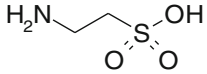	2.19	<2

structures. Protonation states for the desired pH of 7 were generated manually by editing the 3D structures and the ligands were energy minimized using the CFF force-field.

For docking studies we decided to use the LigandFit software of Accelrys [21]. Preliminary docking calculations with AutoDock [22], DOCK [23], eHiTS [24], FlexX [25], GOLD [26], and LigandFit to reproduce the pose of the bound leucine in the leucine transporter $LeuT_{Aa}$ showed that LigandFit was the best software to reproduce the orientation of the leucine in the active site and especially the interaction of the Leucine carboxyl group with the sodium atom Na1.

LigandFit does a Monte Carlo conformational search to generate ligand conformations suitable for docking. For the generation of ligand conformers a distance dependent dielectric constant of 80 is used to mimic an aqueous environment. During the conformational search, bond length and bond angles of the ligand remain constant. A ligand/site shape matching occurs to select ligand conformations that are similar to the shape of the active site. The selected ligand conformations are positioned in the binding site, including multiple orientations. Rigid body energy minimization of the candidate pose using the DockScore energy function is performed and the best poses are saved. Afterward, the energy of the docked ligand and the protein atoms within a distance of 8 Å around the ligand are minimized using steepest descent and later conjugate gradient methods without any position restraining (flexible docking). The energy grid used for the docking procedure was calculated using the CFF force-field. The Jain scoring function [27] was used to compare the docking results with measured pIC50 values for mGAT-1 (Table 1).

Results and discussion

For this study we focused on the generation of three-dimensional models for hGAT-1 suitable for docking and virtual screening experiments. The modeled hGAT-1 3D structure contains 516 residues, showing 12 transmembrane helices and the helices TM1 and TM6 unwound in the region of the active site, very similar to $LeuT_{Aa}$. Forty-four residues on the N-terminus and 33 on the C-terminus of hGAT-1 were discarded because no alignment with the significantly shorter sequence of $LeuT_{Aa}$ was found. After homology model building and preliminary docking of GABA into the active site a force-field based minimization with fixed backbone atoms of the homologue was performed. The quality of the minimized hGAT-1 protein achieved in this way was very good with only five residues displaying unfavored Phi and Psi angles in the Ramachandran plot (Fig. 2) and 92.7% of the residues in the preferred regions. The five residues in disallowed

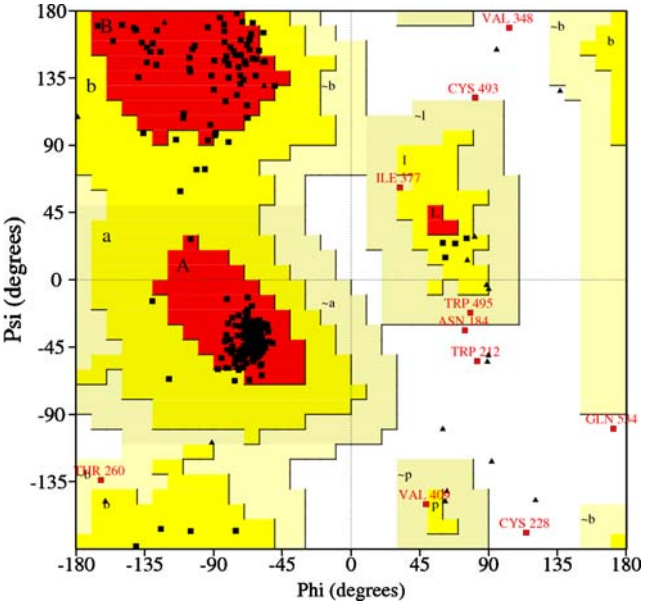

Fig. 2 Ramachandran plot of the GAT-1 model. The most favored regions are colored red, additional allowed, generously allowed, and disallowed regions are indicated as yellow, light yellow and white fields, respectively; 92.7% of the residues are in most favored regions

regions are all more than 15 Å apart from the active site. It is therefore unlikely that they might influence the docking calculations. Profiles-3D showed very good quality scores for all internal residues of the hGAT-1 model (Fig. 3). Scores for residues on the surface normally interacting with the lipophilic membrane are varying strongly between very well and poor. This is a drawback of the Profiles-3D method which was designed for cytosolic proteins [19] and not for membrane proteins. However, the good Profiles-3D scores for the active site and the residues

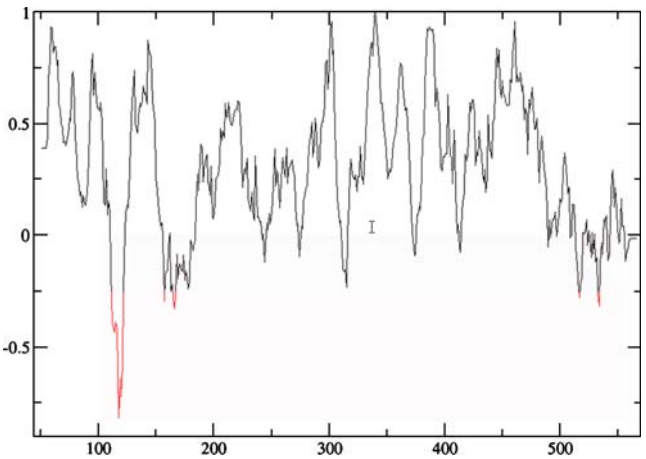

Fig. 3 Profiles-3D verify score for GAT-1 residues. Regions with low verify score (plotted in red) belong to intracellular loop IL1, extracellular loop EL2, and TM11, respectively

directly surrounding it show clearly the validity of the active site of our hGAT-1 model.

As indicated by Yamashita et al. [7], the bound leucine in the $LeuT_{Aa}$ structure is coordinated by various polar contacts (Fig. 4a). The carboxy group of the bound leucine is part of an H-bond network with the backbone-NH from Leu25 and Gly26, the side-chain-OH of Tyr108, and the sodium atom Na1. The amino group interacts with the backbone carbonyl-oxygens of Ala22, Phe253, Thr254, and the side-chain-OH of Ser256. The lipophilic end of the bound leucine interacts with Val104, Tyr108, Phe253, Phe259, and Ile359, of which only Ile359 is shown in Fig. 4a.

GABA binding mode

Using LigandFit and the described flexible docking procedure led to a single binding mode of GABA into hGAT-1. As outlined below, this binding mode appeared to be well suited to appropriately predict the score values for a set of known test compounds without the need to investigate an additional binding mode as published recently [10]. Our binding mode shows a high degree of similarity for the binding of the carboxylic end of GABA as compared to that of leucine in the $LeuT_{Aa}$ structure (Fig. 4b). Accordingly, the carboxylic end of GABA is bound to one of the sodium atoms present (Na1) and fixed in a network of hydrogen bonds encompassing the side-chain-OH of Tyr140 and the backbone-NH of Leu64 and Gly65, analogical to the way the carboxy end of leucine is bound in $LeuT_{Aa}$. Previously, based on differences in amino acids lining the active site a "cyclic" binding conformation has been suggested for GABA [28]. Unlike this speculation, the carbon chain of GABA adopts an extended conformation shifting the position of the NH group of GABA by 4.03 Å in comparison to that of leucine NH. Furthermore, the GABA NH forms a different set of hydrogen bonds which now includes the side-chain-OH of Thr400, side-chain-OH of Ser396 and, to a minor extent, with the side-chain-OH of Tyr60 and the backbone-O of Tyr60 and Ser396.

The different substrate specificity of hGAT-1 compared to $LeuT_{Aa}$ is based mainly on the three mutations between $LeuT_{Aa}$ to hGAT-1 (Ser256 to Gly297, Asn21 to Tyr60, Ile359 to Thr400), changing the hydrogen bonding pattern and electrostatics in the active site (Fig. 4b). The important hydrogen bond acceptors in $LeuT_{Aa}$ Ser256 and Asn21 interacting with the NH of the bound leucine are replaced by Gly297 and Tyr60 in hGAT-1, respectively. On the side of the binding domain diagonally across from the aforementioned amino acids the lipophilic interaction of Ile359 is replaced by Thr400, offering a new hydrogen bond interaction in the correct distance for the GABA-NH.

Estimation of hGAT-1 activity

As reference for the docking experiments performed in this study experimental binding data were used that had been obtained from the same test system, a biological assay based on the murine GABA transporter mGAT-1 published by us [29]. This represents a clear advantage, as variations of the binding data as a result of different binding assays can be excluded. Furthermore, because of the high similarity between mGAT-1 and hGAT-1 (98% identity; 99.17% similarity according to BLOSUM100 scoring matrix) the biological data from mGAT-1 can be considered to closely resemble those for hGAT-1 and to be a valid substitute for the latter. This is even truer, as all amino acids located in or close to the active site are identical.

The Jain scoring function was chosen because after flexible docking as described above it allows a direct

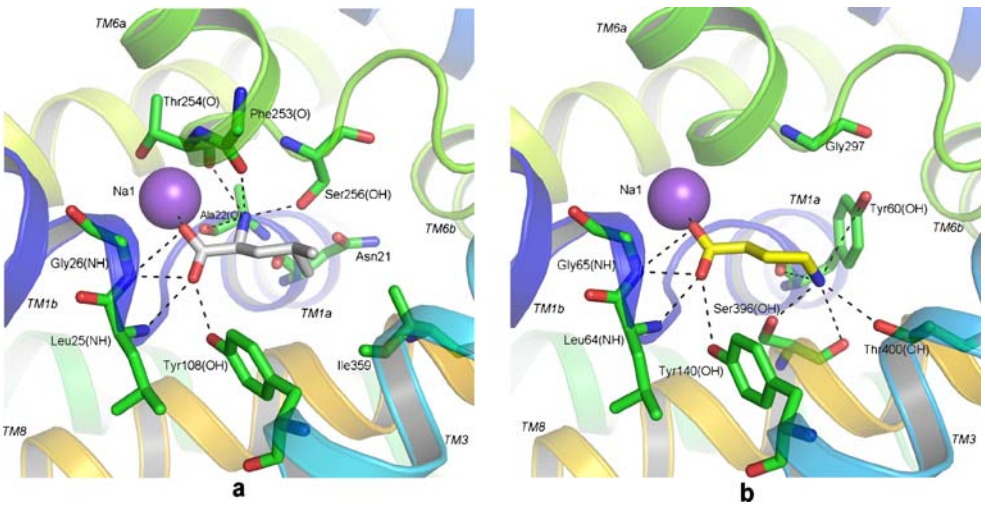

Fig. 4 (**a**) Polar interactions of Leucine and $LeuT_{Aa}$. Trans-membrane helices TM10, TM11, TM12, and side-chain of Phe253 are not shown for clarity. Numbering is for $LeuT_{Aa}$; (**b**) Polar interactions of GABA and GAT-1. Trans-membrane helices TM10, TM11, and TM12 are not shown for clarity. Numbering is for hGAT-1

estimation of the activity of the selected ligands without any further refinement or molecular dynamics simulation.

The rank order of potency for GABA uptake inhibition is modeled very well (Table 1). Well-known potent uptake inhibitors like GABA, (*R*)-nipecotic acid, 4-amino-crotonic acid and (*S*)-4-amino-2-hydroxybutanoic acid (Table 1, Entries 1, 2, 3, and 5) are clearly identified though the activity of the later compound is a little overestimated. The scoring values of compounds with low potency like β-alanine, 4-amino-isocrotonic acid and taurine, (Table 1, Entries 11, 10, and 12) are in good agreement with the biological data. Notwithstanding that the scoring values of guvacine (Table 1, Entry 4) and (*S*)-nipecotic acid (Table 1, Entry 7) are too low, our model is able to differentiate the subtle differences between (*R*)-nipecotic acid and (*S*)-nipecotic acid (pIC50 of 5.074 versus 4.126, Jain score of 4.94 versus 3.3), 4-amino-crotonic acid and 4-amino-isocrotonic acid (pIC50 of 4.975 versus 2.986, Jain score of 4.83 versus 2.5). Also the activities of medium potent inhibitors like β-proline and (*S*)-homoproline (Table 1, Entries 6 and 9) are accurately predicted. In the biological test (*R*)-homoproline (Table 1, Entry 8) is slightly more active than its (*S*) analogue, (Table 1, Entry 9). Although the better binding enantiomer is correctly predicted by the scoring function, its activity is overestimated by more than an order of magnitude.

Conclusions

Homology modeling of human hGAT-1 using the 3D structure of $LeuT_{Aa}$ as template and careful energy minimization lead to a high quality 3D structure of hGAT-1. This structure provides insights into the binding mode of GABA and related compounds. The different substrate selectivity of hGAT-1 compared to $LeuT_{Aa}$ can be explained mainly by the exchange of three residues in the active site (Ser256 to Gly297, Asn21 to Tyr60, Ile359 to Thr400). These mutations lead to a substantial change of the hydrogen bonding pattern at the amino end of the substrate and a significant increase of the distance between binding areas for the carboxy and the amino end of GABA as compared to leucine as substrate, allowing an extended conformation of bound GABA. The exchange of Ile359 with a threonine (Thr400) and Ser 296 with a glycine (Gly297) are considered to be major reasons for GABA selectivity since due to these mutations a H-bond acceptor is shifted into the lipophilic part of the active site which in $LeuT_{Aa}$ interacts with the lipophilic side chain of Leucine.

The hGAT-1 homology structure is well suited for docking hGAT-1 inhibitors with a molecular weight below 250, as calculations using our in-house data showed. Flexible docking in combination with the Jain scoring function allows the estimation of potential GABA uptake inhibition without any additional refinement using molecular dynamics calculations. The rank order of potency of selected compounds is very well reproduced and even subtle differences, e.g. between different stereoisomers like (*R*)- and (*S*)-nipecotic acid can be calculated.

The active site is closed and of very limited size and it is neither accessible from the extra- nor the intra-cellular side preventing the docking of larger hGAT-1 inhibitors. This ‘double-closed’ structure of the protein was already pointed out by Yamashita et al. [7] for the $LeuT_{Aa}$ structure. Molecular dynamics calculations or even better a 3D crystal structure with a larger bound inhibitor are necessary to gain more detailed insights into the transport of GABA through the membrane and to investigate possible inhibition mechanisms in more detail.

References

1. Nelson H, Mandiyan S, Nelson N (1990) FEBS Lett 269:181–184
2. Borden LA, Smith KE, Hartig PR, Branchek TA, Weinshank RL (1992) J Biol Chem 267:21098–21104
3. Guastella J, Nelson N, Nelson H, Czyzyk L, Keynan S, Miedel MC, Davidson N, Lester HA, Kanner BI (1990) Science 249:1303–1306
4. Masson J, Sagné C, Hamon M, Mestikawy SE (1999) Pharmacol Rev 51:439–464
5. Chen N, Reith MEA, Quick MW (2004) Pflugers Arch 447:519–531
6. Gether U, Andersen PH, Larsson OM, Schousboe A (2006) Trends Pharmacol Sci 27:375–383
7. Yamashita A, Singh SK, Kawate T, Jin Y, Gouaux E (2005) Nature 437:215–223
8. Dodd JR, Christi DL (2007) J Biol Chem 282:15528–15533
9. Beuming T, Shi L, Javitch JA, Weinstein H (2006) Mol Pharmacol 70:1630–1642
10. Palló A, Bencsura A, Héja L, Beke T, Perczel A, Kardos J, Simon A (2007) Biochem Biophys Res Commun 364:952–958
11. Boeckmann B, Bairoch A, Apweiler R, Blatter M, Estreicher A, Gasteiger E, Martin MJ, Michoud K, O'Donovan C, Phan I, Pilbout S, Schneider M (2003) Nucleic Acids Res 31:365–370
12. Bernstein FC, Koetzle TF, Williams GJB, Meyer EF Jr, Brice MD, Rodgers JR, Kennard O, Shimanouchi T, Tasumi M (1977) J Mol Biol 112:535–542
13. Sali A, Blundell TL (1993) J Mol Biol 234:779–815
14. van der Spoel D, Lindahl E, Hess B, Groenhof G, Mark AE, Berendsen HJC (2005) J Comput Chem 26:1701–1718
15. Hess B, Kutzner C, van der Spoel D (2008) Lindahl E 4:435–447
16. Scott WRP, Hunenberger PH, Tironi IG, Mark AE, Billeter SR, Fennen J, Torda AE, Huber T, Kruger P, van Gunsteren WF (1999) J Phys Chem A 103:3596–3607
17. Essmann U, Perera L, Berkowitz ML, Darden T, Lee H, Pedersen LG (1995) J Chem Phys 103:8577–8592
18. Laskowski RA, MacArthur MW, Moss DS, Thornton JM (1993) J App Cryst 26:283–291

19. Lüthy R, Bowie JU, Eisenberg D (1992) Nature 356:83–85
20. Maple JR, Hwang MJ, Stockfisch TP, Dinur U, Waldman M, Ewig CS, Hagler AT (1994) J Comput Chem 15:162–182
21. Venkatachalam CM, Jiang X, Oldfield T, Waldman M (2003) J Mol Graph Model 2:289–307
22. Morris GM, Goodsell DS, Halliday RS, Huey R, Hart WE, Belew RK, Olson AJ (1998) J Comput Chem 19:1639–1662
23. Moustakas DT, Lang PT, Pegg S, Pettersen E, Kuntz ID, Brooijmans N, Rizzo RC (2006) J Comput-Aided Mol Design 20:601–619
24. Zsoldos Z, Reid D, Simon A, Sadjad SB, Johnson AP (2007) J Mol Graph Model 26:198–212
25. Rarey M, Kramer B, Lengauer T, Klebe G (1996) J Mol Biol 261:470–489
26. Jones G, Willet P, Glen RC, Leach AR, Taylor R (1997) J Mol Biol 267:727–748
27. Jain AN (1996) J Comput-Aided Mol Design 10:427–440
28. Kanner B, Zomot E (2008) Chem Rev 108(5):1654–1668
29. Kragler A, Höfner G, Wanner KT (2008) Eur J Med Chem 43:2404–2411